

# Microstructured silver surfaces produced by freeze casting for enhanced phase change heat transfer

G J Gouws<sup>1</sup> and N Shortt

School of Engineering and Computer Science, Victoria University of Wellington,  
Wellington, New Zealand

E-mail: gideon.gouws@vuw.ac.nz

**Abstract.** Microporous silver surface layers were formed on copper substrates by means of a modified freeze casting method. The structure of such layers is the result of the templating action of the ice crystals and layers were found to contain a hierarchical porous structure. Three different pore morphologies were present in the microstructure with pore sizes ranging from approximately 0.5 to 200  $\mu\text{m}$ . The application of these surface structures was found to considerably enhance the heat flux during the nucleate phase of pool boiling, with heat fluxes up to five times higher from a microporous surface compared to a bare copper substrate. Bubble formation and departure was found to be significantly different on the two types of surfaces, with smaller bubbles formed with a high density on the microporous surface. The enhancement in heat flux by these structures is most likely due to the combined effect of an increased surface area with high thermal conductivity, an increase in nucleation sites for bubble formation as well as effective wicking from micropores to sustain bubble growth and departure.

## 1. Introduction

Materials with a porous microstructure play an important role in enhancing many energy related processes and technologies such as batteries, fuel cells, supercapacitors and catalysts [1]. These structures not only provide a large surface area, but potentially also increase the density of reaction sites to augment the energy transfer process. In the case of a phase change heat transfer process such as pool boiling, the use of porous or structured surfaces is the primary mechanism that can be used to enhance the heat flux or to delay the onset of a critical heat flux [2]. Several methods for the fabrication of such surfaces can be found in the literature, ranging from sintering of small particles to self-assembly or microfabrication [3].

This paper presents the fabrication of porous silver microstructured surfaces on copper substrates by a modified freeze casting process. The technique is a relatively simple and inexpensive method to produce a hierarchical porous surface structure with control over pore dimensions and alignment. In addition to the pore structure, these layers also have a large surface area and high thermal conductivity and thus have the potential for application in many different energy transfer and storage processes. The efficacy of these surfaces in enhancing heat transfer during the early nucleate phase of pool boiling will be evaluated.

---

<sup>1</sup> To whom any correspondence should be addressed.



Freeze casting has gained popularity over the last decade as a method for preparing porous microstructures with a high degree of pore alignment [5,6]. The basic process as illustrated in figure 1 consists of making a colloidal suspension of nano- or micro particles in a solvent (typically water) together with dispersants and binders. This solution is then subjected to a directional freeze, which causes the nucleation of ice crystals (a). These ice crystals grow and propagate through the colloid in the form of hexagonal platelets (b). Any impurities will be rejected by the advancing ice front, and should be trapped in spaces between the ice platelets. At completion of the freeze process, the ice crystals can be removed by sublimation, leaving a porous structure as defined by the templating of the ice crystals (c). The remaining structure can then be annealed to burn off the binder, sinter the particles and produce a denser and mechanically robust structure (d). The resultant pore morphology can be controlled to a degree by a variation of process parameters such as the freeze rate, particle size and shape or the chemical nature of binders and additives.

Using variations of the basic freeze casting method, many workers have shown the preparation of porous ceramic, metal or polymer structures. Applications of material produced by the method have mostly focussed on potential biomaterials such as tissue or bone scaffolds [7,8], drug delivery scaffolds [9] or ultrasound tissue phantoms [10]. The potential uses of these structures in porous electrode materials and in fuel cells have also been suggested [11].

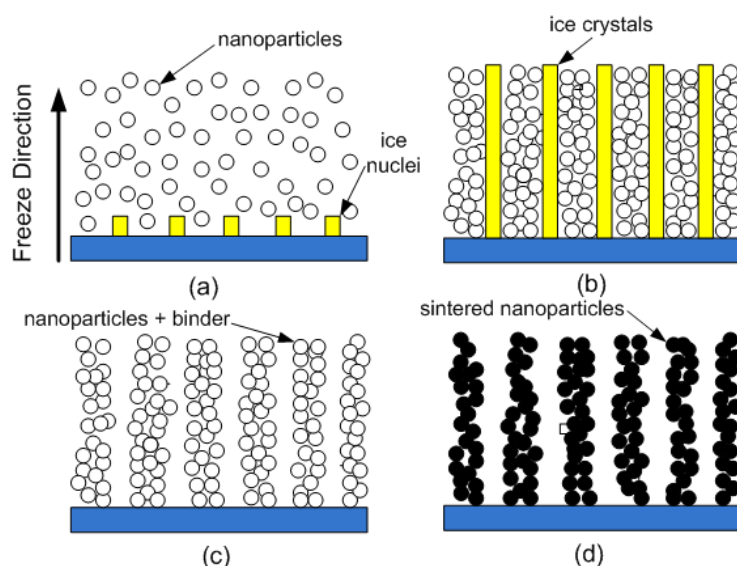


**Figure 1:** The idealised formation of a porous structure by a freeze cast process. A colloidal suspension of nanoparticles is subjected to a temperature gradient to initiate freezing (a) and the growing ice crystals reject any impurities (b). The ice can be removed in a sublimation step (c) after which an anneal step is used to sinter the nanoparticles and improve mechanical strength (d).

## 2. Experimental Method

Silver nanoparticles with diameters between 100 – 500 nm were used as the starting material. Colloidal suspensions were made by slowly dispersing the nanoparticles in a 1% solution of polyvinyl alcohol in water, producing mass loadings of nanoparticles from 10% to 40%. Vortex mixing and ultrasonic disruption were used to prevent particle aggregation and promote dispersion.

Substrates in the form of copper discs with a typical thickness of 2.5 mm and a diameter of 25 mm were machined, degreased in acetone and isopropanol and given a final etch in acetic acid to remove surface oxides. A measured volume of the silver nanoparticle colloidal solution was then dispensed on the substrate and the substrate placed on top of a copper cold finger. A small hole in the base of the substrate allowed access to a thermocouple for temperature measurement during the freeze cast step as well as later during heat transfer tests. The temperature of the cold finger was controlled by Peltier thermoelectric elements and a controlled ramp from room temperature to  $-40\text{ }^{\circ}\text{C}$  was induced in the cold finger.

At the conclusion of the freeze step, samples were removed from the cold finger and placed in a vacuum freeze drier for a period of  $\sim 48$  hours, after which samples were annealed in a tube furnace under inert gas flow for 4 hours at a temperature of  $500^\circ\text{C}$ .

The efficacy of the films in enhancing heat transfer during the nucleate phase of pool boiling was investigated by mounting the samples on the top of a copper heat flux finger that was heated from the bottom by cartridge heaters. The sample was then fitted into the bottom of a glass boiling vessel containing saturated, pre-boiled deionised water at atmospheric pressure as the working liquid. By measuring the temperature profile along the heat flux finger as well as the surface temperature of the copper substrate, the heat flux as a function of excess temperature  $\Delta T_{\text{ex}}$  ( $\Delta T_{\text{ex}} = T_{\text{surface}} - T_{\text{saturation}}$ ) was calculated for values of  $\Delta T_{\text{ex}}$  in the range  $0 - 10^\circ\text{C}$ . A camera was fitted at the top of the test system enabling viewing of the sample surface during the process.

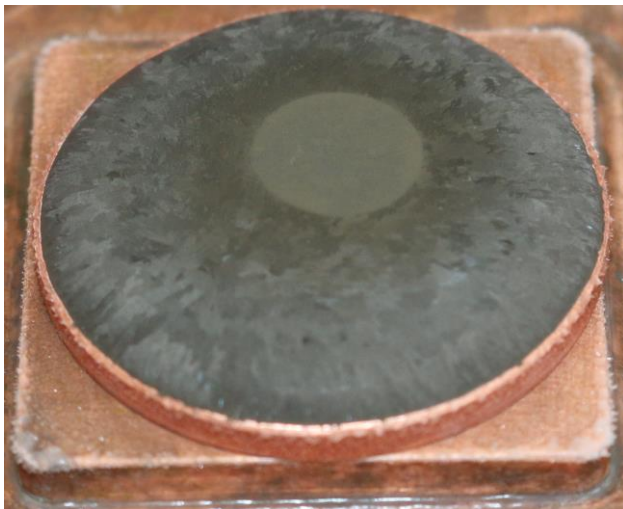


**Figure 2:** A copper substrate with Ag nanoparticle colloid on a cold finger during the freeze step. Freezing proceeds from the outside inwards and the position of the freeze front can be seen as the circular ring.

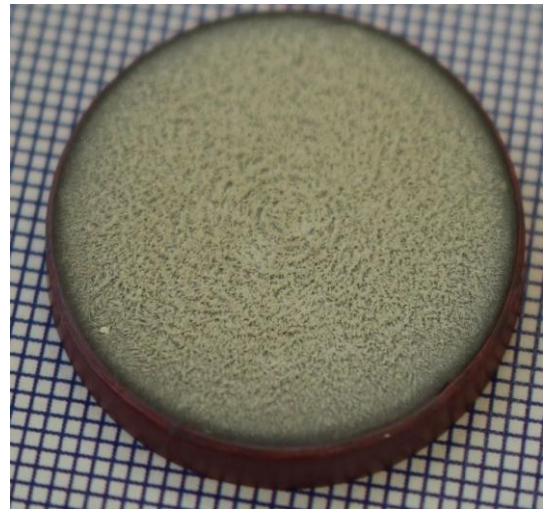


**Figure 3:** The appearance of the porous silver layer at the completion of the anneal step to remove the polymer binder and sinter the Ag nanoparticles.

### 3. Material Microstructure

The appearance of the silver surface after annealing is shown in figure 3, while the detailed microstructure structure is presented at different length scales in figure 4. It is found that the structure increases in density from the outside perimeter of the substrate to the centre, i.e. in the direction of the freeze front. This is consistent with particles and other impurities being ejected by the advancing ice front and eventually concentrating in the centre of the sample. This effect is least noticeable in samples with high Ag particle mass loadings or when very high freeze rates were used and may be due to the fact that in these cases the moving freeze front was unable to reject particles, leading to a more even structure over the substrate.

Studying the microstructure in more detail in the SEM (figure 4) allows the observed pores to be broadly divided into three types based on their shape and size:

**Type A:** Relatively large ( $\sim 100$  to  $200\ \mu\text{m}$ ) irregular shaped pores that are relatively randomly distributed through the structure (figure 4(a)).

**Type B:** Elongated porous channels separated by nanoparticle walls, with channels typically  $40$  to  $80\ \mu\text{m}$  in length and approximately  $10\ \mu\text{m}$  wide (figure 4(b)). The walls consist of sintered nanoparticles as was ejected by the ice crystals and have a typical thickness of  $5$  to  $10\ \mu\text{m}$ . These channels and walls are found to be aligned over small areas ( $0.2$  to  $0.5\ \text{mm}^2$ ) of the sample.

**Type C:** Micropores form within the nanoparticle walls, as these walls are not densely packed. These pores have typical dimensions of  $0.5 - 5 \mu\text{m}$ . Figure 4(c)

The observed pore structure was found to be weakly dependant on the freeze rate, with higher freeze rates leading to the preferential formation of Type A and C pores at the expense of Type B. This is to be expected, as high freeze rates will produce smaller ice crystals with fast moving fronts which will destroy the periodic nature of the Type B pores. It can also be assumed that the circular tool marks on the substrate acts as nucleation points for ice platelets and as such it will be difficult to produce structures with better alignment of the walls and channels without more elaborate surface preparation.

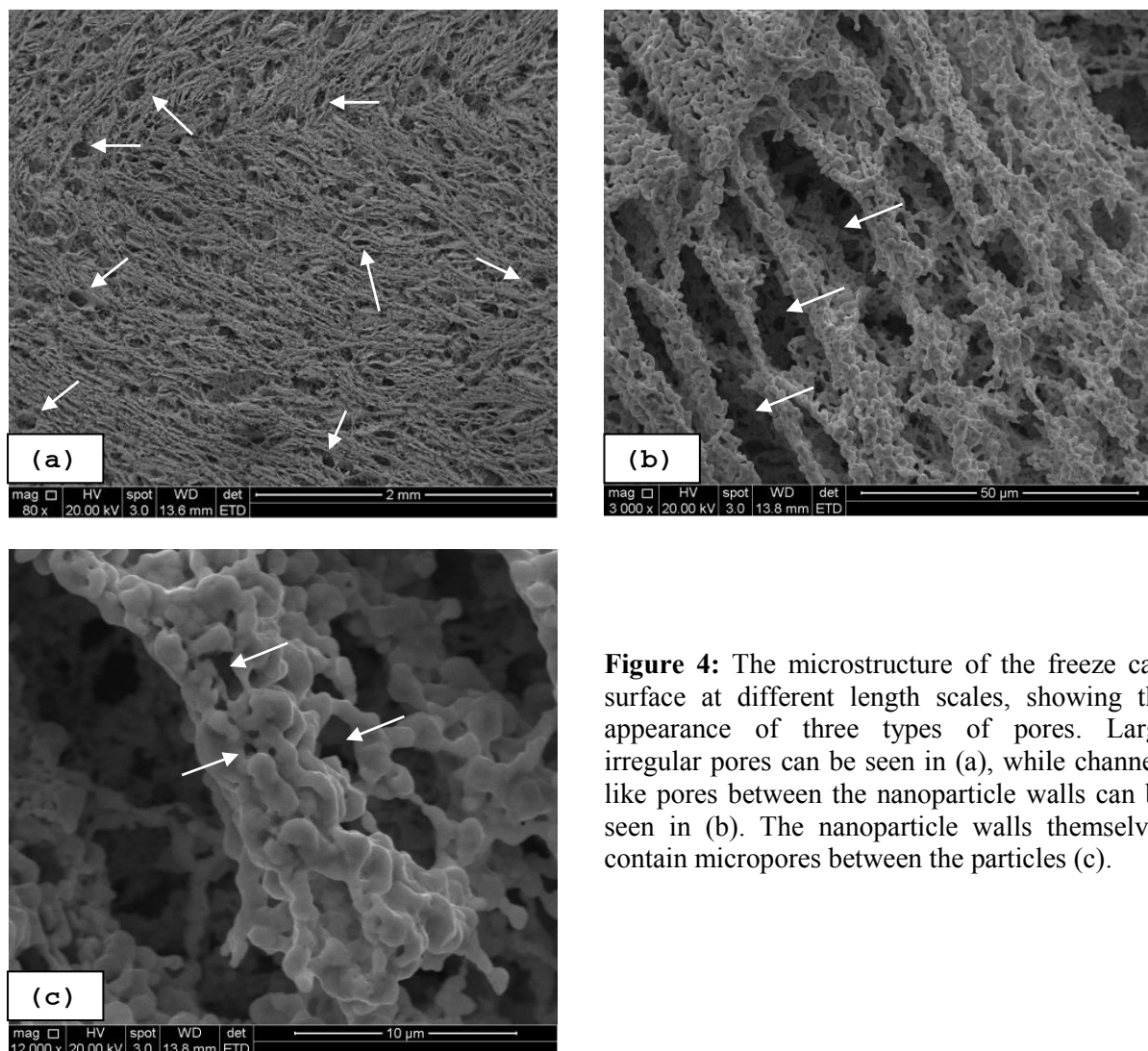


**Figure 4:** The microstructure of the freeze cast surface at different length scales, showing the appearance of three types of pores. Large irregular pores can be seen in (a), while channel-like pores between the nanoparticle walls can be seen in (b). The nanoparticle walls themselves contain micropores between the particles (c).

#### 4. Boiling heat transfer measurements

The results from heat flow during pool boiling on the porous silver surface were compared to that from on a standard Cu substrate with no surface layer (Figure 5). Very little difference in the heat flux from the different samples were noted at low values of excess temperatures ( $\Delta T_{\text{ex}} < 2^\circ\text{C}$ ). For the bare copper substrate, the heat flux increased relatively slowly until  $\Delta T_{\text{ex}} \sim 5.5^\circ\text{C}$ , after which a sharp increase in the heat flux is observed. In the case of a microporous layer present on the surface, this departure from the initial low value of heat flux occurs at much lower values of  $\Delta T_{\text{ex}}$ ; ranging



from approximately  $\Delta T_{\text{ex}} = 2.5$  °C for a 10% Ag mass loading to  $\Delta T_{\text{ex}} = 1.8$  °C for a 40% Ag mass loading. It is interesting to note that the performance of samples with a mass loading of 10 – 30 % Ag are comparable, but the 40% mass loading has significantly better heat transfer. At an excess temperature of  $\Delta T_{\text{ex}} = 8$  °C the first three samples produced a heat flux that was approximately 3.3 times that of the copper substrate, while the 40% silver sample had a heat flux 5.3 times that of the copper.

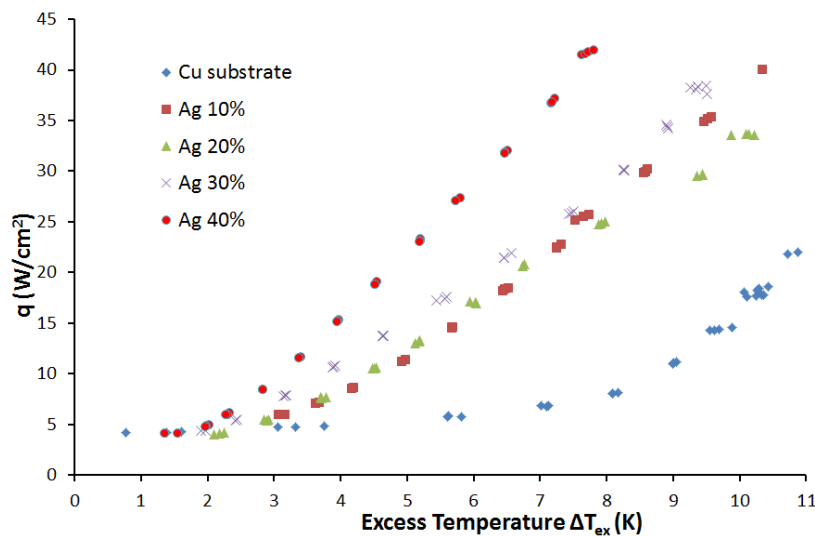


**Figure 5:** The heat flux from porous surfaces with different Ag mass loadings as a function of excess temperature  $\Delta T_{\text{ex}}$  compared to that observed on a bare copper substrate.

The formation of bubbles and their departure was found to be significantly different on the two types of surfaces at these low values of excess temperature. Bubbles that form on the machined copper surface at  $\Delta T_{\text{ex}}$  of  $\sim 2$  °C (figure 6) had an average diameter of  $0.41 \pm 0.16$  mm, while at similar temperatures on the porous silver surfaces (figure 7) a mean bubble diameter of  $0.28 \pm 0.08$  mm was observed. The density of bubbles was also significantly higher on porous surface, with a typical density of 24 bubbles/cm<sup>2</sup> on the copper surface compared to approximately 80 bubbles/cm<sup>2</sup> on the porous surfaces. In the latter case, low contrast between bubbles and surface makes clear identification harder and together with the smaller size of the bubbles it may well lead to an underestimation of bubble density. Significant bubble departure from the microstructured surface also occurs well in advance from that on the copper surface, in agreement with the point of increase in the heat flux observed for the different samples.

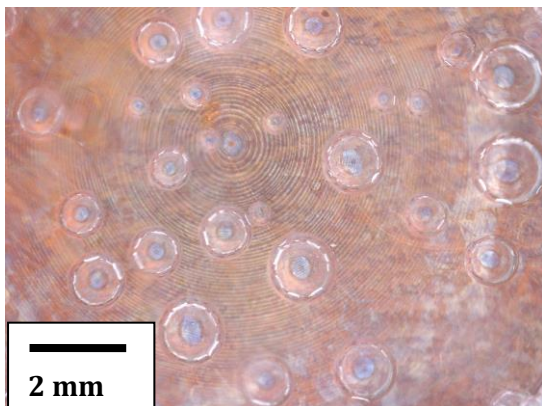


**Figure 6:** Bubble formation at  $\Delta T_{\text{ex}} \sim 2$  °C on a bare copper substrate.

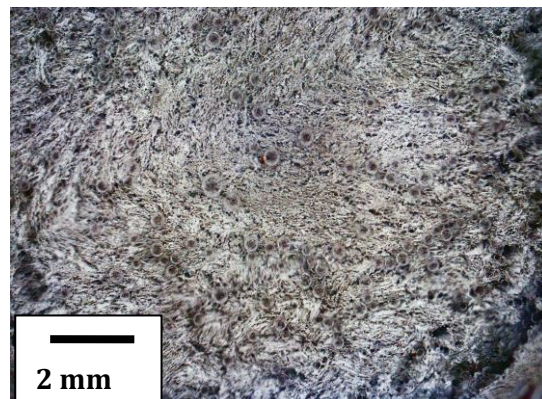


**Figure 7:** Bubble formation at  $\Delta T_{\text{ex}} \sim 0.8$  °C on a microporous Ag surface.

The different types of pores in the structure may potentially each play a role in contributing to the enhanced heat flux. Both the Type A and B pores will enhance the number of potential nucleation sites. Due to their channel shape with a high aspect ratio, the Type B pores may also contribute to an upward squirt or jet effect during bubble departure as was suggested by Wang [12]. This has the potential to further enhance fluid convection during the release of bubbles. The micropores in the walls may play a role in feeding liquid to the growing bubbles and sustain the process, while at the same time the high thermal conductivity of the silver nanoparticles as well as the associated high surface area of the porous structure will be effective in transferring heat from the copper surface into the fluid.

## 5. Summary

Porous surface structures were prepared from silver nanoparticles using a modified freeze cast method. Three different types of pores could be identified, with pore sizes spanning three orders of magnitude. The surfaces were evaluated for the enhancement of heat transfer during the early nucleate stage of pool boiling and heat fluxes up to five times higher than that from a standard machined copper surface was obtained. Bubble densities increased on the microporous surfaces, together with significantly higher departure rates at lower values of excess temperature. The roles played by different types of pores from the structure in enhancing the heat flux needs further study in order to understand the mechanisms of heat transfer enhancement and optimise the microstructure.

## References

- [1] Li Y, Fu Z and Su B 2012 Hierarchically Structured Porous Materials for Energy Conversion and Storage *Adv. Funct. Mater.* **22** 4634
- [2] Attinger D, Frankiewicz C, Betz A R, Schutzius T M, Ganguly R, Das A, Kim C and Megardis C M 2014 Surface Engineering for Phase Change Heat Transfer: A Review *MRS Energy and Sustainability* **1** E4
- [3] Patil C M and Kandlikar S G 2014 Review of the Manufacturing Techniques for Porous Surfaces Used in Enhanced Pool Boiling *Heat Transfer Engineering* **35**(10) 887
- [4] Lu Y and Kandlikar S G 2011 Nanoscale Surface Modification Techniques for Pool Boiling Enhancement – A Critical Review and Future Directions *Heat Transfer Engineering* **32**(10) 827
- [5] Deville S, Saiz E, Nalla R K and Tomsia A P 2006 Freezing as a Path to Build Complex Composites *Science* **311** 515
- [6] Deville S 2008 Freeze-Casting of Porous Ceramics: A Review of Current Achievements and Issues *Advanced Engineering Materials* **10**(3) 155
- [7] Pawelek K M, Husmann A, Best S M and Cameron R E 2014 Ice-templated structures for biomedical tissue repair: From physics to final scaffolds *Applied Physics Reviews* **1** 021301
- [8] Deville S 2010 Freeze-Casting of Porous Biomaterials *Materials* **3** 1913
- [9] Gutiérrez M C, García-Carvajal Z Y, Jobbágy M, Rubio F, Yuste L, Rojo F, Ferrer M L and Del Monte F 2007 Poly(vinyl alcohol) Scaffolds with Tailored Morphologies for Drug Delivery and Controlled Release *Adv. Funct. Mater.* **17** 3505
- [10] Dawson A, Harris P, Gouws G J 2010 Anisotropic Microstructured Poly(Vinyl Alcohol) Tissue-Mimicking Phantoms *IEEE Transactions on Ultrasonics, Ferroelectrics and Frequency Control* **57**(7) 1494
- [11] Chen Y, Bunch J, Li T, Mao Z and Chen F 2012 Novel functionally graded acicular electrode for solid state cells fabricated by the freeze-tape-casting process *Journal of Power Sources* **213** 93
- [12] Wang X S, Wang Z B and Chen Q Z 2010 Research on Manufacturing Technology and Heat Transfer Characteristics of Sintered Porous Surface Tubes *Advanced Materials Research* **97-101**, 1161